Available online at www.sciencedirect.com
SCIENCE DIRECT®
Tectonophysics 383 (2004) 193–215
TECTONOPHYSICS
www.elsevier.com/locate/tecto

Thermotectonic evolution of the Ukrainian Donbas Foldbelt: evidence from zircon and apatite fission track data

C. Spiegel[a], R.F. Sachsenhofer[b,*], V.A. Privalov[c], M.V. Zhykalyak[d], E.A. Panova[e]

[a] *School of Earth Sciences, University of Melbourne, 3010 Victoria, Australia*
[b] *Institut für Geowissenschaften, Montanuniversität Leoben, Abt. Mineralogie und Petrologie, Universitat Leoben, Peter-Tunner-Strasse, A-8700 Leoben, Austria*
[c] *Donetsk National Technical University, Artem Str. 58, UA-83000 Donetsk, Ukraine*
[d] *Donetsk State Regional Geological Survey, Sybirtseva Str. 17, UA-84500 Artemovsk, Ukraine*
[e] *UkrNIMI, National Academy of Science of Ukraine, Tchelyuskintsev Str. 291, UA-83121 Donetsk, Ukraine*

Received 8 April 2003; accepted 16 March 2004

Abstract

The Donbas Foldbelt forms part of a large Devonian rift cross-cutting the southern part of the Eastern European Craton. It comprises a 20-km-thick Devonian and Carboniferous sedimentary succession. Maximum burial occurred during early Permian time and was followed by a major exhumation phase. In this study we use zircon and apatite fission track dating to reconstruct the post-depositional thermal evolution of the inverted basin. Modelling of the fission track data, combined with modelling of vitrinite reflectance data, reveals that large parts of the basin were affected by a Permo-Triassic (~ 250 Ma) heat flow event, which was presumably related to Permo-Triassic andesitic magmatism. This Permo-Triassic thermal event was predicted by previous modelling of vitrinite reflectance data, but only the fission track data indicates its wide areal distribution. Probably large parts of the southern margin of the Eastern European Craton were affected by this event. Whereas rocks west of the city of Donetsk (Krasnoarmeisk Monocline) experienced Permo-Triassic temperatures in the range of 90–105 °C, rocks northwest of Donetsk were heated to up to more than 240 °C. Jurassic temperatures northeast of Donetsk were in the order of 90–100 °C. These relatively high temperatures imply that a significant part of the Carboniferous sequence became eroded only during early Cretaceous times and/or that the Jurassic heat flow was significantly increased (~ 90 mW/m^2). Elevated heat flows may be related to Jurassic magmatic activity. Sediments in the southern Donbas Foldbelt (Yuzhno–Donbassky region) and the westernmost Krasnoarmeisk Monocline record cooling below 60 °C during Jurassic times, whereas samples northeast of Donetsk cooled below 60 °C during Cretaceous times. A correlation between this last cooling and the present-day depths of the samples suggests that the main episode of folding along the South Syncline and the South Anticline pre-dates Cretaceous cooling.

Keywords: Apatite fission track; Zircon fission track; Thermal history; Dniepr–Donets Basin; Thermal modelling; Magmatism

1. Introduction

The Donbas (Donets Basin) forms part of a large intracratonic paleorift cross-cutting the southern part

* Corresponding author. Tel.: +43-3842-402-6104; fax: +43-4842-402-6102.
E-mail address: sachsenh@unileoben.ac.at (R.F. Sachsenhofer).

0040-1951/$ - see front matter © 2004 Elsevier B.V. All rights reserved.
doi:10.1016/j.tecto.2004.03.007

of the Eastern European Craton in a WNW–ESE direction. The Donbas is located between the Dniepr–Donets Basin and the buried Karpinsky Swell (Fig. 1).

The basin fill of the Donbas contains Devonian pre- and syn-rift rocks with a maximum thickness of 6 km along the basin axis and a Carboniferous post-rift sequence with a preserved thickness of 13–14 km (Maystrenko et al., 2003; Fig. 1). Unlike other segments of the rift, the Donbas experienced phases of severe relief formation and tectonic inversion (e.g. Saintot et al., 2003a,b). Therefore, the structure of the basin is dominated by WNW–ESE trending anticlines and synclines (Donbas Foldbelt), which are the sur-

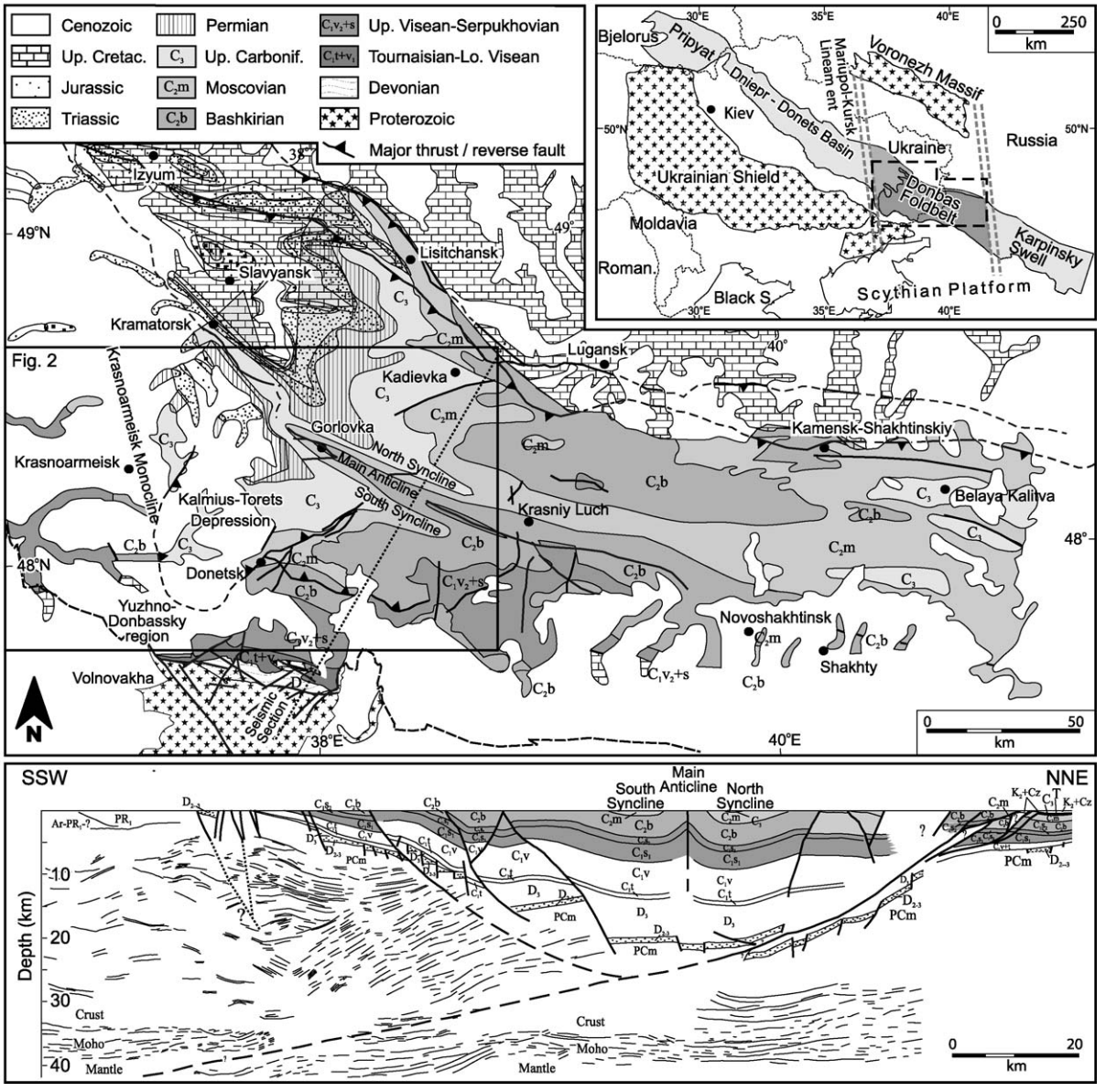

Fig. 1. Location of the study area and geologic sketch map of the Donets Basin (modified after Popov, 1963). Geological cross-section after Maystrenko et al. (2003) and Saintot et al. (2003a,b).

face expression of a crustal-scale pop-up structure (Maystrenko et al., 2003). The age of compressional deformation is a matter of controversy. Both, dominantly Permian and dominantly late Cretaceous ages have been proposed. Another important compressional phase occurred during late Triassic to early Jurassic times (see Stephenson et al., 2001 for a discussion).

The Carboniferous succession hosts approximately 130 coal seams, each with a thickness over 0.45 m. Coal rank is generally high and reaches the meta-anthracite stage. Low-rank coals are restricted to the western and northern basin margins (Levenshtein et al., 1991; Sachsenhofer et al., 2002), where the rank is controlled mainly by temperatures attained during deep Permian burial. The resulting coalification pattern was overprinted in some areas by thermal events probably related to magmatic intrusions, presumably of late Permian age (Sachsenhofer et al., 2002).

In the present paper zircon and apatite fission track (FT) data are presented to provide additional information on the thermotectonic history of the basin, which is a key region for understanding the evolution of the southern margin of the Eastern European Craton. The main aim of the study is to constrain the timing of thermal events which affected the Donets Basin and overprinted coalification patterns in the Ukrainian part of the basin. In addition, the fission track ages will contribute to the understanding of basin evolution and foldbelt formation.

2. Geological setting

2.1. Basin structure

Important information on the deep structure of the Donbas Foldbelt, which is the inverted part of the Dniepr–Donets Basin, is provided by the "DOBRE" refraction (Grad et al., 2003) and reflection lines (Maystrenko et al., 2003). The structure of the central basin is dominated by WNW–ESE trending folds (Fig. 1). Major thrusts occur along the northern margin of the basin. Minor folds, reversed faults and rotated fault blocks prevail along the southern boundary of the basin. The age of thrusting and folding is a matter of controversy:

Following traditional ideas, Privalov et al. (1998) assume a dominantly Permian age, which is also corroborated by new results from deep wells. According to Privalov et al. (2002) 90–98% of the 1.5–2.9 km displacement on reactivated thrusts along the northern basin margin, between Lugansk and Kamensk Shakhtinskiy, occurred during Permian time. Late Triassic to early Jurassic and late Cretaceous compressional activities locally affected the northwestern (Izyum–Lugansk), northeastern (NNE Belaya Kalitva; Popov, 1963, Nagorny, 1971; Privalov et al., 1998), and southeastern margins of the Donbas Foldbelt (S of Novoshakhtinsk; Belokon, 1975), and the southwestern rim of the Kalmius–Torets Depression (Popov, 1963).

In contrast, Stovba and Stephenson (1999) and Saintot et al. (2003a,b), based on seismic evidence and microtectonic data, favour a Permian transtensional phase and a dominantly late Cretaceous age for the main compressional event. According to Saintot et al. (2003b), the formation of the Main Anticline was initiated in Permian times by active salt movements.

The southwestern part of the Donbas comprises the Krasnoarmeisk Monocline and the Kalmius–Torets Depression. The eastern margin of the Kalmius–Torets Depression is formed by a set of NE-trending faults, which may be the surface expression of the deep Donetsk–Kadievka basement fault zone (Belokon, 1975; Fig. 2). The area east of the city of Donetsk is dominated by WNW–ESE trending folds including the Main Anticline, the South Syncline and the South Anticline (Fig. 2).

2.2. Basin evolution

2.2.1. Devonian syn-rift phase

Main rifting occurred during the middle/late Devonian (e.g. van Wees et al., 1996). The total thickness of Devonian pre- and syn-rift rocks exposed along the southern margin of the Donets Basin is 750 m, including thick volcanic rocks (McCann et al., 2003; Fig. 3). The thickness of Devonian rocks along the basin center reaches up to 6 km. After a period of tectonic quiescence, tectonic extension was reactivated during the late early Visean (Saintot et al., 2003b).

2.2.2. Late Paleozoic post-rift phase

Major post-rift subsidence occurred during the Permo-Carboniferous. The coal-bearing Carbonifer-

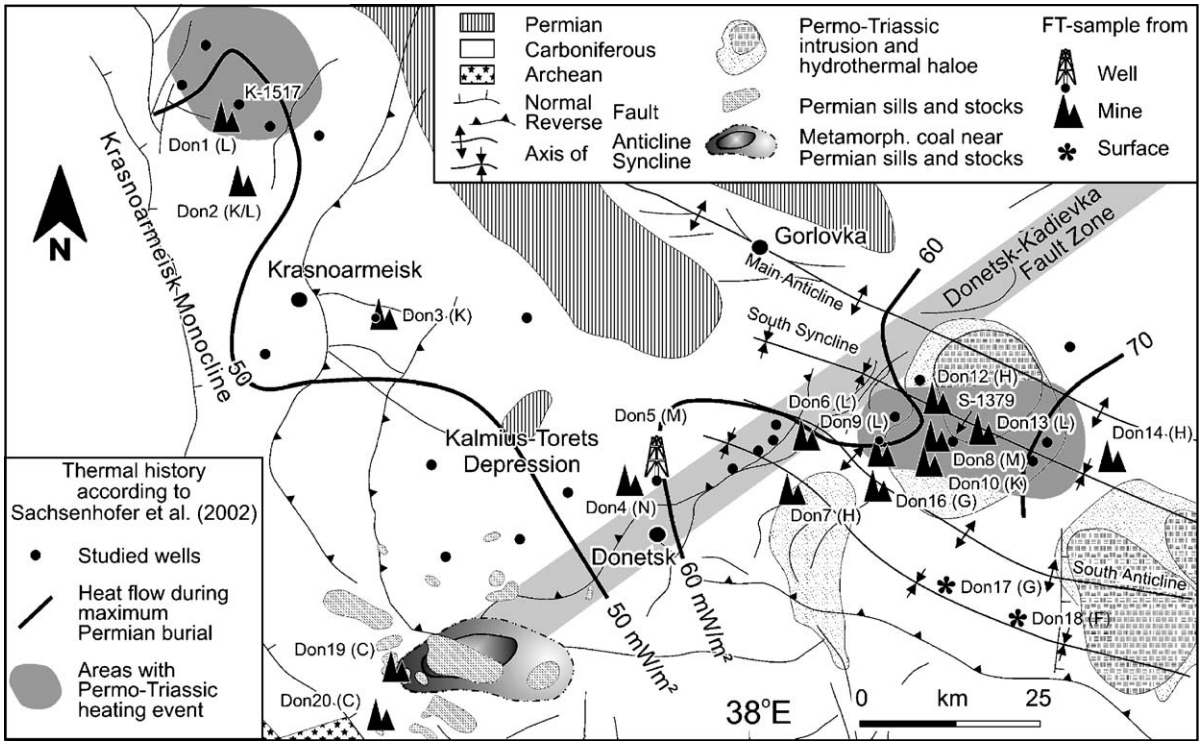

Fig. 2. Position of studied fission track samples (Don 1 to Don 20; see Fig. 1 for location of map). Letters in parenthesis refer to Carboniferous suites. Some aspects of the thermal history of the basin are indicated according to Sachsenhofer et al. (2002). Isolines show the heat flow distribution during maximum Permian burial. Areas with a Permo-Triassic heat flow event north of Krasnoarmeisk and east of Donetsk are highlighted by grey shading. The position of intrusive bodies is also indicated (after Popov, 1966; Aleksandrov et al., 1996).

ous sequence, up to 14 km thick, is subdivided into lithostratigraphic units named suites A, B, C, to P (Lutugin and Stepanov, 1913). Their correlation with the standard time-scale is presented in Fig. 3. Deposition ages used here are according to this lithostratigraphy. Permian rocks, up to 2.5 km thick, are preserved along the western margin of the Donbas. Permian rocks with a thickness of up to 250 m were also drilled in the region of the northern marginal faults of the Donets Basin north of Belaya Kalitva (Nesterenko, 1978). Maximum burial in the central basin occurred during Sakmarian times (~ 275 Ma; e.g. Sachsenhofer et al., 2002; Izart et al., 2003). However, exhumation may have started slightly earlier (~ 285 Ma?) along the Main Anticline and in the Yuzhno–Donbassky and Krasnoarmeisk regions (Saintot et al., 2003b; S. Stovba, personal communication).

2.2.3. Permian exhumation

Within the Donbas Foldbelt Permian rocks and significant parts of the Carboniferous sequence were eroded during a major Permian exhumation phase, reflected by a basin-wide unconformity. Uplift and exhumation may be related to the build-up of stress emanating from the Hercynian Caucasus/Uralian orogens or to the activity of an asthenospheric diapir (e.g. Sollogub et al., 1977; Gavrish, 1989; Chekunov, 1994).

Using 1D and 2D numeric models, Sachsenhofer et al. (2002) estimated Permian erosion to be in the order of 2–3 km in the Krasnoarmeisk Monocline and the Kalmius–Torets Depression, but 4–6 km east of the Donetsk–Kadievka fault zone. Low vitrinite reflectance values (0.6–0.7% Rr; Sachsenhofer et al., 2003) indicate that erosion in the Yuzhno–Donbassky region was minor. Nagorny and Nagorny (1976) as-

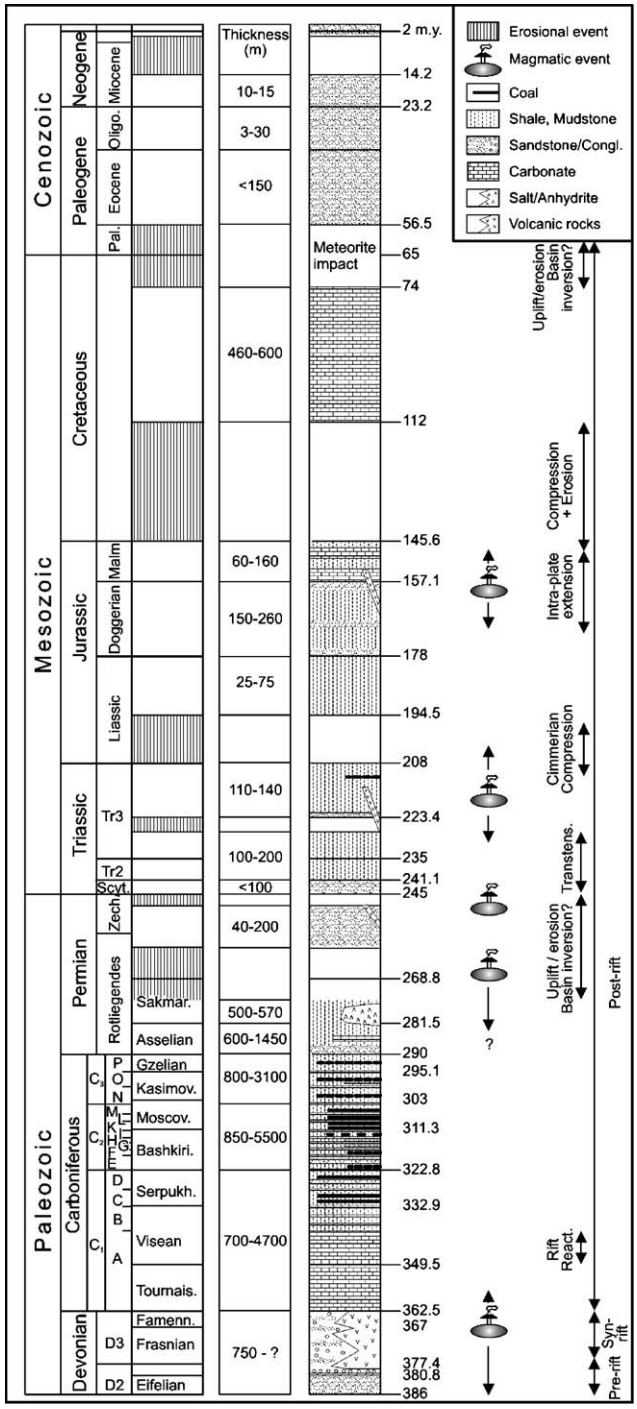

Fig. 3. Chrono- and lithostratigraphy of the Donets Basin. Major magmatic and tectonic events are also shown (Sterlin et al., 1963; Belokon, 1971; Einor, 1996; Privalov et al., 1998; Stovba and Stephenson, 1999). Time-scale after Harland (1990).

sumed erosion of as much as 15 km along the southern basin margin (S′ of Novoshakhtinsk), as much as 11 km in the central part of the basin, and about 2 km along the northern basin margin, implying a pronounced asymmetry of Permian exhumation. Stovba and Stephenson (1999) suggested erosion of up to 10 km within the Ukrainian Shield based on extrapolations of missing strata in view of seismic evidence.

Many authors assumed that the main basin inversion (compressional deformation) occurred during Permian uplift (e.g. Popov, 1963; Nagorny and Nagorny, 1976; Mikhalyev, 1976; Privalov, 1998). In contrast, Stovba and Stephenson (1999) and Saintot et al. (2003a,b) assumed that Permian uplift and exhumation occurred during a period of (trans)tensional reactivation. The latter authors speculated that salt movements related to (trans)tension initiated the formation of the Main Anticline.

While extensive syn-rift magmatism occurred in most of the Dniepr–Donets Basin, post-rift magmatic rocks have been described only in the Donets Basin. These include Permian (~ 280–270 Ma) alkaline rocks southwest of Donetsk (Fig. 3; e.g. Lazarenko et al., 1975, Alexandre et al., 2003), which probably intruded during early basin uplift (e.g. Buturlinov, 1964; Privalov et al., 1998).

2.2.4. Mesozoic–Cenozoic post-rift phase

The post-rift phase was characterised by relatively thin unconformity-bounded sedimentary sequences (Fig. 3). Magmatic events produced early (250–245) and late Triassic (230–200 Ma) (trachy-)andesites and dacites and Jurassic (~ 155 Ma) lamprophyres (e.g. Lazarenko et al., 1975, de Boorder et al., 1996, Privalov, 2000, Alexandre et al., 2003; Fig. 3). Using magnetic data, deep seismic sounding data and field observations, Aleksandrov et al. (1996) mapped large hidden intrusions and their hydrothermal haloes in the western Donets Basin. The authors advocate for a late Permian (Triassic?) age of the intrusion. The locations of the postulated intrusive bodies are shown in Fig. 2.

Several compressional events with different siginificance affected the Donets Basin during Triassic/Jurassic (Cimmerian) times and are well established, e.g. in the area between Lugansk and Lisitchansk (for location, see Fig. 1; Popov, 1963; Nagorny, 1971; Privalov, 1998).

An early Cretaceous (pre-Aptian) exhumation phase affected the southeastern basin margin (Pogrebnov, 1971; Belokon, 1971, 1975; Privalov, 1998). An important compressional event recorded in different parts of the Donbas Foldbelt occurred during late Cretaceous to early Tertiary time (Popov, 1963; Privalov, 1998). According to Stovba and Stephenson (1999) and Saintot et al. (2003a,b), this event caused main folding and thrusting.

2.3. Permian–early Triassic heat flow history

Using 1D and 2D numerical models, Sachsenhofer et al. (2002) reconstructed the heat flow history of the Ukrainian Donets Basin. According to these models, heat flow during maximum (Permian) burial was in the range of 40–75 mW/m^2 (Fig. 2).

High surface heat flow after maximum burial occurred along the South Syncline (up to 200 mW/m^2) and in the northern Krasnoarmeisk Monocline (up to 150 mW/m^2) and was probably related to (Permo-Triassic?) magmatic intrusions. Age and location of the area with high heat flow in the South Syncline fit well with the magmatic intrusions postulated by Aleksandrov et al. (1996; Fig. 2). In contrast, no magmatic activity is known from the Krasnoarmeisk region yet.

Reconstructed paleo-heat flows southwest of Donetsk (Yuzhno–Donbassky region) are rather low. This is remarkable because in this area Carboniferous coal sequences have been contact metamorphosed by Permian sills and stocks (Jernovaya, 1997; Fig. 2).

3. Fission track analysis—results and discussion

3.1. Sample description

Twenty Carboniferous sandstone samples were chosen for FT analysis. Seventeen samples were taken in coal mines, one was derived from a borehole, and two additional samples were taken from outcrops (Table 1). For sample locations see Fig. 2; analytical procedures are described in Appendix A. Eighteen samples yielded sufficient apatite for FT analysis. Vitrinite reflectance (VR, see Table 1) was measured on samples from nearby coaly layers following established procedures (Taylor et al., 1998). According to

Table 1
Apatite fission track and vitrinite reflectance data

Sample no.	Mine	Lithology	Stratigraphic age (Ma)	Depth (mbs)	Temperature (°C)	Ro (%)	Maximum paleotemperature	Counted grains	U content (ppm)	Spontaneous		Induced		$P\chi^2$ (%)	Dosimeter		Central age (Ma ± 1σ)	Measured H.C.T.	Mean length (μm ± 1σ)	S.D. (μm)
										ρ_s	n_s	ρ_i	n_i		ρ_d	n_d				
Krasnoarmeisk Monocline																				
DON1	Belozerskaya	sandstone	307	405	22	n.m.	–	20	22	19.80	1143	17.18	992	48	10.68	3732	236 ± 12	101	13.51 ± 0.18	1.82
DON2	Dobropolskaya	sandstone	308	462	23	0.9/0.78	120–150	20	23	20.04	663	17.59	582	43	10.89	3732	238 ± 15	100	12.04 ± 0.26	2.60
DON3	Dimitrova	sandstone	309	357	21	0.79	120–135	20	29	25.72	642	22.48	561	8	11.07	3732	242 ± 18	100	11.98 ± 0.22	2.21
Folds east of Donetsk																				
DON4	Butovskaya	sandstone	303	800	30	0.83	125–140	20	26	14.34	603	18.67	785	7	11.27	3732	167 ± 12	101	11.51 ± 0.31	3.07
DON5	Borehole Sch-1352 (73)	sandstone	304	1250	49	n.m.	–	20	21	13.13	504	18.52	711	<1	11.46	3732	164 ± 14	86	11.16 ± 0.35	3.26
DON6	Yasinofskaya Glubokaya	sandstone	307	715	30	1.49	165–180	20	21	13.20	676	19.67	1007	79	11.66	3732	151 ± 8	100	12.13 ± 0.29	2.85
DON7	Kirov Makeevugol	sandstone	313	480	24	n.m.	–	20	16	11.59	494	16.12	687	9	11.86	3732	174 ± 13	100	12.92 ± 0.26	2.58
DON8	Rassvet	sandstone	305	617	22	2.10	190–205	20	32	18.66	535	26.23	752	13	12.05	3732	166 ± 11	100	12.23 ± 0.28	2.79
DON9	Zhdanovskaya	sandstone	308	570	21	2.19	195–210	20	27	14.93	577	24.01	928	83	12.25	3732	147 ± 9	100	11.76 ± 0.28	2.83
DON10	Ternopol'skaya	sandstone	309	404	13	2.92	220–230	12	28	18.93	344	25.14	457	85	12.44	3732	180 ± 14	50	12.42 ± 0.37	2.60
DON12	Poltavskaya	sandstone	313	480	18	2.60	205–225	18	17	9.70	447	16.30	751	99	12.64	3732	145 ± 9	73	11.95 ± 0.34	2.91
DON13	Komsomolets Donbassa	sandstone	307	810	29	n.m.	–	20	35	16.41	584	32.43	1154	98	12.83	3732	125 ± 7	100	11.77 ± 0.29	2.87
DON14	Severnaya	sandstone	315	540	19	4.54	≫250 °C	19	18	10.83	520	18.10	869	91	13.03	3732	150 ± 9	97	12.52 ± 0.33	3.21
DON16	Kommunist Novaya	sandstone	317	474	18	n.m.	–	20	31	18.80	326	29.17	506	93	12.66	3816	157 ± 12	100	11.94 ± 0.31	3.07
DON17	Stephano-Krinkvil	sandstone	317	0	10	n.m.	–	14	22	16.42	268	19.98	326	98	12.91	3816	204 ± 17	78	12.73 ± 0.35	3.07
DON18	Blagodatov	sandstone	320	0	10	n.m.	–	6	19	13.49	126	17.44	163	96	13.15	3816	195 ± 24	16	13.92 ± 0.41	1.65
Yuzhno–Donbassky region																				
DON19	Y-Donbasskaya3	sandstone	330	827	31	0.73	115–130	20	21	22.75	332	20.97	306	98	13.40	3816	277 ± 23	100	11.58 ± 0.28	2.78
DON20	Y-Donbasskaya1	sandstone	330	350	21	0.57	90–105	20	20	21.88	252	20.92	241	97	13.64	3816	272 ± 25	100	12.31 ± 0.31	3.14

Fission track ages were calculated using dosimeter glasses CN5 with ζCN5 = 390 ± 6. Dating was performed according to the external detector method (Gleadow, 1981) and the zeta calibration approach (Hurford and Green, 1983).

n = number of counted tracks, ρ = track density ($\times 10^5$ tracks/cm^2).

Temperatures refer to present-day mine temperatures at the sampled depth level, paleotemperatures were calculated from the VR data after Burnham and Sweeney (1989) for two different heating rates (0.5 and 50 °C/Ma).

$P\chi^2$ is the probability of obtaining χ^2 value for v degrees of freedom (where v = number of crystals − 1).

Abbreviations: mbs = meters below surface, Ro = vitrinite reflection, H.C.T. = horizontal confined track, S.D. = standard deviation, n.m. = not measured. Mines, boreholes and outcrops are all situated at elevations between 200 and 250 m above sea level.

VR data all analysed samples (except Don 20) experienced post-depositional temperatures high enough to reset the apatite FT system (total annealing temperature for fluor-apatite = 110 °C, Gleadow and Duddy, 1981). Furthermore, VR data suggests that one sample (Don 14) was also reset with regard to the zircon FT system (closure temperature ~ 240 °C, Hurford, 1986). Paleotemperatures were calculated after Burnham and Sweeney (1989) and are listed in Table 1.

3.2. Zircon FT dating

In addition to Don 14 we chose samples Don 17 and Don 18 for Zr FT analysis. No own VR data are available for these two samples, but according to coalification maps (Levenshtein et al., 1991) they may have experienced similar post-depositional temperatures as Don 14.

Don 17 and Don 18 yield central Zr FT ages of 322 Ma and 314 Ma, respectively, which is in the range of their stratigraphic ages (Table 2; Fig. 4). Therefore, these ages are interpreted as partially reset mixed ages. Don 14, in contrast, yields a central age of 249 Ma. This is in good agreement with a late Permian (257–248 Ma) intrusion-related heat flow event postulated by Sachsenhofer et al. (2002) on the basis of numeric models calibrated with VR trends.

3.3. Apatite FT dating

Apatite FT ages and mean track lenghts are listed in Table 1. Confined track length distributions are shown in Fig. 5. FT ages differ significantly depending on sample location:

- The three samples from the *Krasnoarmeisk Monocline* (Don 1–3) yield early to mid-Triassic FT ages between 242 and 236 Ma.
- All samples from the *folds east of Donetsk* (Don 4–18) show Jurassic ages, except one sample (Don 13) which has an early Cretaceous FT age. The two outcrop samples reveal early Jurassic ages (195 and 204 Ma) and are therefore older than the subsurface samples (180–145 Ma, middle to late Jurassic ages).
- The two samples from the *Yuzhno–Donbassky region* (area SW Donetsk; Don 19–20) yield early Permian FT ages (277 and 272 Ma).

Table 2
Zircon fission track data

Sample no.	Mine	Lithology	Stratigraphic age (Ma)	Depth (mbs)	Temperature (°C)	Ro (%)	Counted grains	U content (ppm)	Spontaneous		Induced		$P\chi^2$ (%)	Dosimeter		Central age (Ma ± 1σ)
									ρ_s	n_s	ρ_i	n_i		ρ_d	n_d	
Folds east of Donetsk																
DON14	Severnaya	sandstone	315	540	19	4.54	20	379	458.28	2825	42.34	261	92	4.05	2798	249 ± 17
DON17	Stephano-Krinkvil	sandstone	317	0	10	n.m.	20	225	341.09	2768	24.89	202	64	4.15	2798	322 ± 25
DON18	Blagodatov Location 2	sandstone	320	0	10	n.m.	20	255	380.04	2491	28.68	188	52	4.19	2798	314 ± 26

Zircon fission track ages were calculated using dosimeter glasses CN2 with ζCN2 = 116 ± 2. Dating was performed according to the external detector method (Gleadow, 1981) and the zeta calibration approach (Hurford and Green, 1983).
n = number of counted tracks, ρ = track density ($\times 10^5$ tracks/cm^2).
Temperatures refer to present-day mine temperatures at the sampled depth level. $P\chi^2$ is the probability of obtaining χ^2 value for v degrees of freedom (where v = number of crystals − 1).
Abbreviations: mbs = meters below surface, Ro = vitrinite reflection, n.m. = not measured.

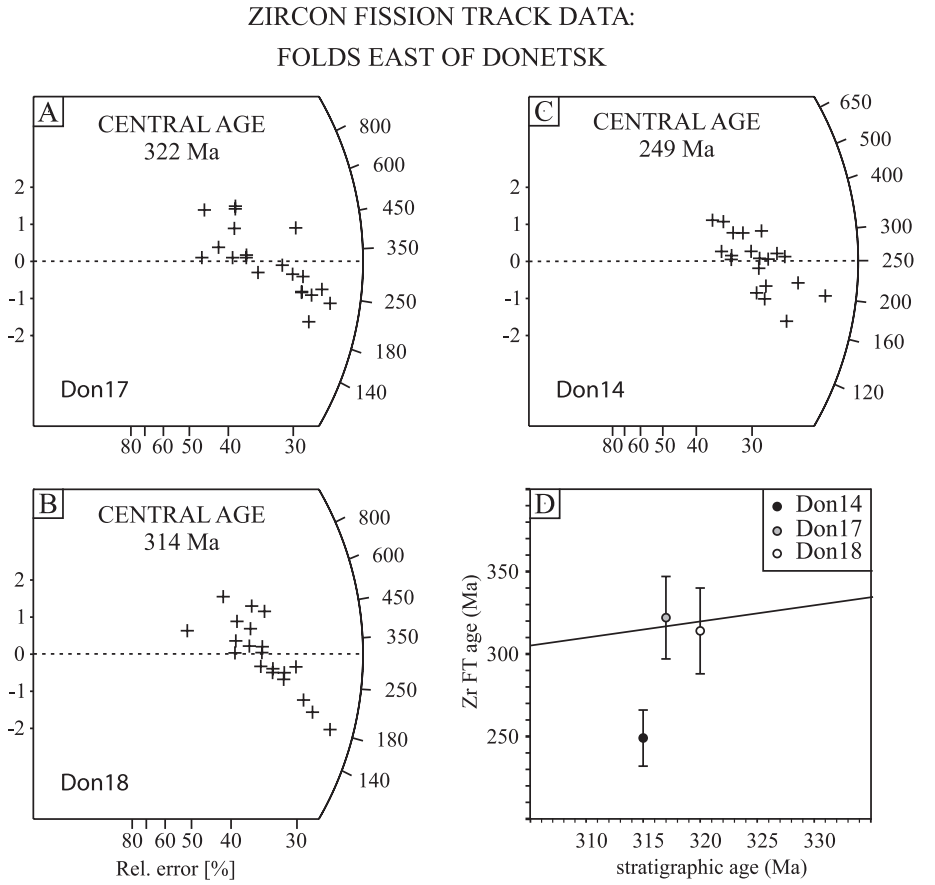

Fig. 4. Radial plots of zircon FT single grain ages for three samples from the folds east of Donetsk (A, B, C), as well as relation between Zr FT central ages and stratigraphic ages of the dated samples (D). Radial plots (Galbraith, 1990) show the precision of the individual grain ages on the *x*-axis (precision increasing to the right). The FT ages of the single grains can be read by extrapolating a line from the origin passing the grain's coordinates and intersecting the age scale on the right side of the plot.

In terms of their track length distributions, samples from the three areas show no significant differences. Mean track lengths and standard deviations of all samples cluster between 11.16 and 13.51 μm and between 1.8 and 3.26 μm, respectively. Track length distributions are unimodal with a tail to shorter lengths. The short mean lengths, high standard deviations and track length distributions point to a complex thermal history with a prolonged stay in the apatite partial annealing zone (PAZ) for all samples.

Fig. 6 shows apatite FT ages plotted against mean track lengths, in a so-called boomerang plot. If samples experienced a single-stage cooling related to a discrete phase of fast denudation, then the plot should form a distinctive boomerang-like pattern (Green, 1986; Gallagher et al., 1998). The samples from the Donets Basin do not show this kind of trend, which again indicates a more complex cooling history.

3.4. Modelling the thermal history

The shortening patterns of fission tracks reflect the cooling paths of rocks through the temperature interval of the apatite partial annealing zone (PAZ, ca. 60–110 °C for fluor-apatite, Gleadow and Duddy, 1981). Hence, FT ages and length distributions can be used as a basis to model thermal histories. In this study, modelling was performed using the AFTSolve program (Ketcham et al., 2000) and the annealing data of

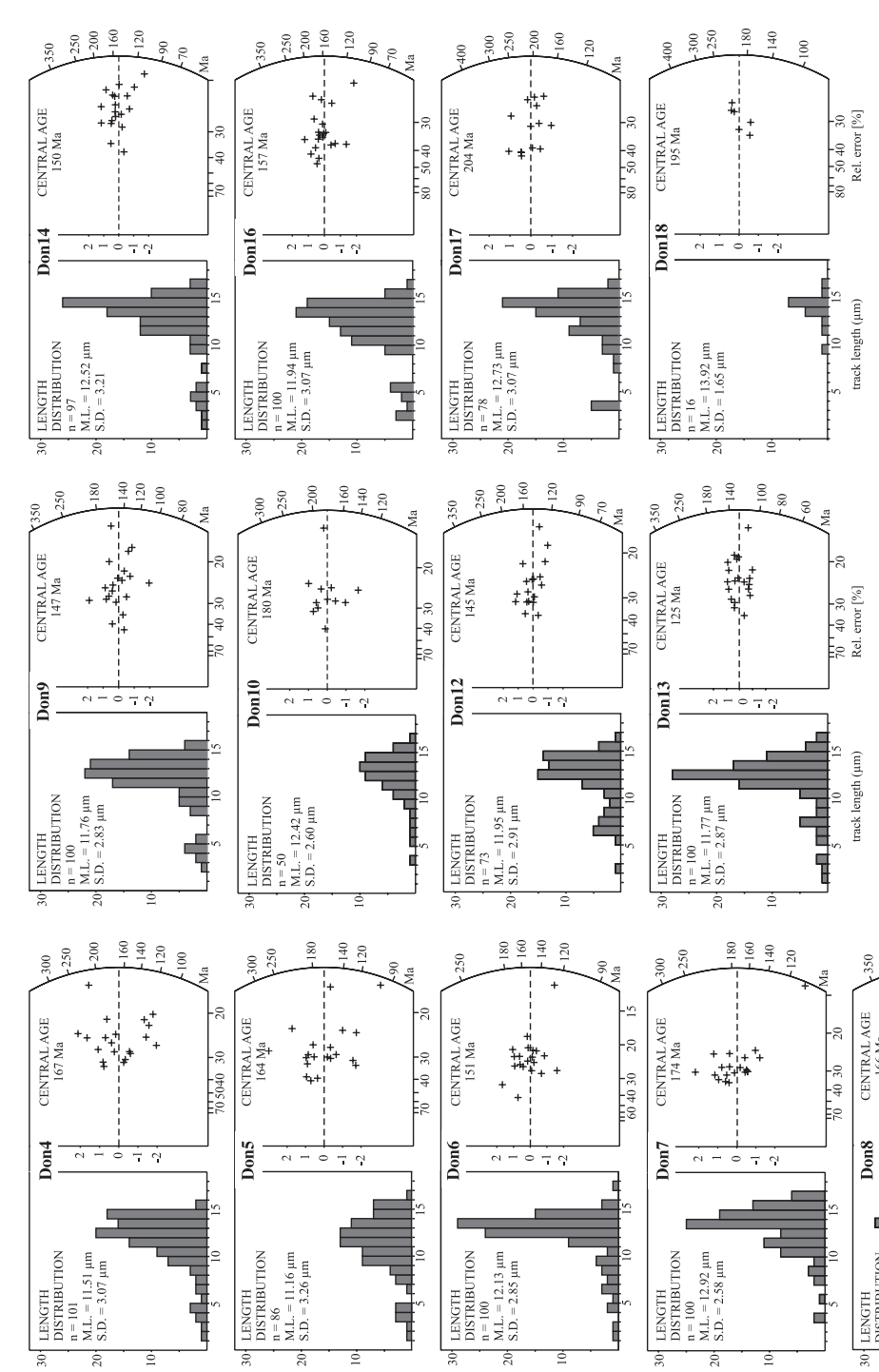
A
APATITE FISSION TRACK DATA - A: FOLDS EAST OF DONETSK
Don4
LENGTH DISTRIBUTION
n = 101
M.L. = 11.51 µm
S.D. = 3.07 µm
CENTRAL AGE
167 Ma
Don5
LENGTH DISTRIBUTION
n = 86
M.L. = 11.16 µm
S.D. = 3.26 µm
CENTRAL AGE
164 Ma
Don6
LENGTH DISTRIBUTION
n = 100
M.L. = 12.13 µm
S.D. = 2.85 µm
CENTRAL AGE
151 Ma
Don7
LENGTH DISTRIBUTION
n = 100
M.L. = 12.92 µm
S.D. = 2.58 µm
CENTRAL AGE
174 Ma
Don8
LENGTH DISTRIBUTION
n = 100
M.L. = 12.23 µm
S.D. = 2.79 µm
CENTRAL AGE
166 Ma
Don9
LENGTH DISTRIBUTION
n = 100
M.L. = 11.76 µm
S.D. = 2.83 µm
CENTRAL AGE
147 Ma
Don10
LENGTH DISTRIBUTION
n = 50
M.L. = 12.42 µm
S.D. = 2.60 µm
CENTRAL AGE
180 Ma
Don12
LENGTH DISTRIBUTION
n = 73
M.L. = 11.95 µm
S.D. = 2.91 µm
CENTRAL AGE
145 Ma
Don13
LENGTH DISTRIBUTION
n = 100
M.L. = 11.77 µm
S.D. = 2.87 µm
CENTRAL AGE
125 Ma
Don14
LENGTH DISTRIBUTION
n = 97
M.L. = 12.52 µm
S.D. = 3.21
CENTRAL AGE
150 Ma
Don16
LENGTH DISTRIBUTION
n = 100
M.L. = 11.94 µm
S.D. = 3.07 µm
CENTRAL AGE
157 Ma
Don17
LENGTH DISTRIBUTION
n = 78
M.L. = 12.73 µm
S.D. = 3.07 µm
CENTRAL AGE
204 Ma
Don18
LENGTH DISTRIBUTION
n = 16
M.L. = 13.92 µm
S.D. = 1.65 µm
CENTRAL AGE
195 Ma
number of horizontal confined tracks
Track length (µm)
track length (µm)
Rel. error [%]
Ma

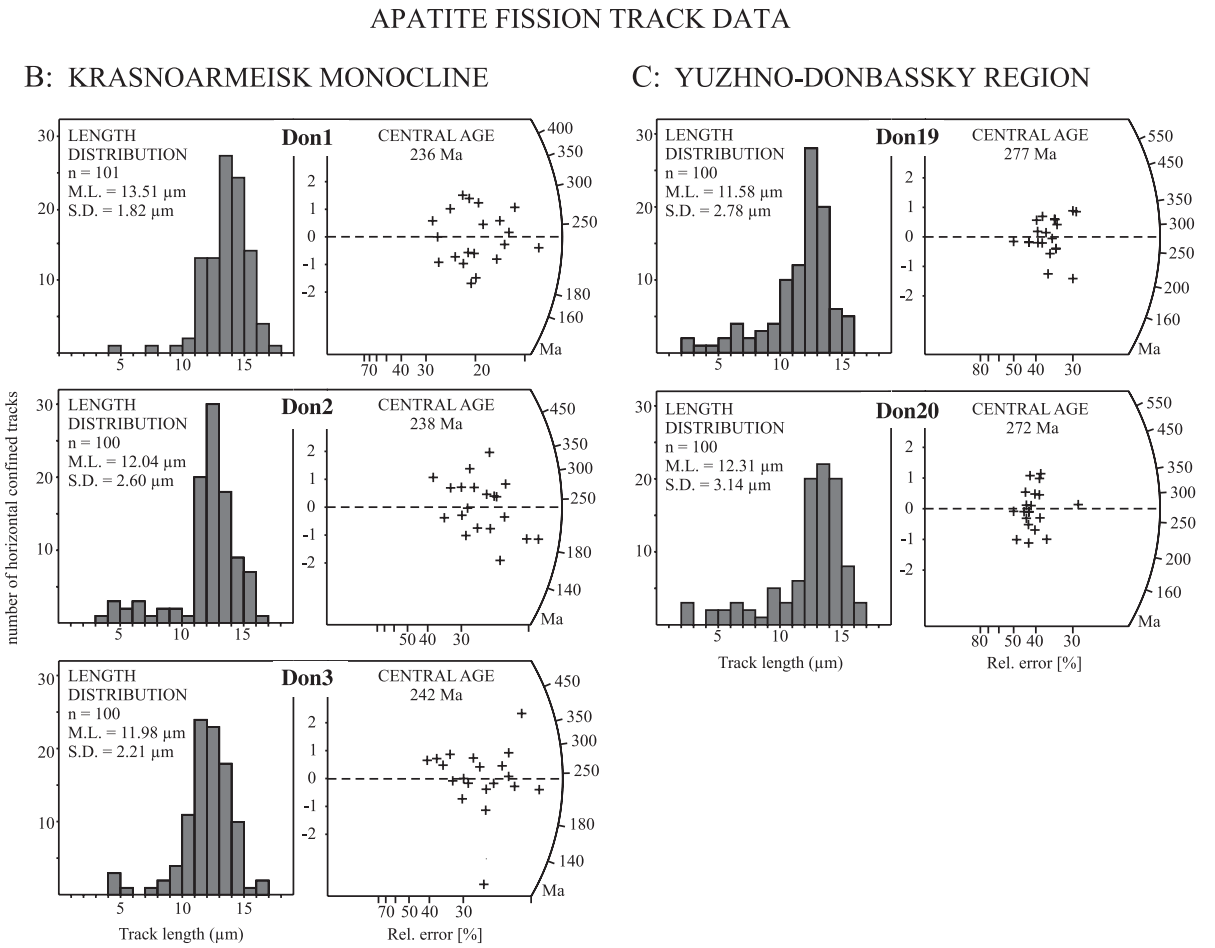

Fig. 5. Length distribution of confined tracks and radial plots displaying apatite FT single grain ages. (A) Samples from the folds east of Donetsk; (B) samples from the Krasnoarmeisk Monocline; (C) samples from the Yuzhno–Donbassky region.

Laslett et al. (1987). Currently, the Laslett et al. (1987) model is by far the most widely used annealing algorithm and has proved to yield reliable estimates of thermal history models. There are, however, some problems associated with this model which will be discussed below.

(1) The chemical composition of apatite, particularly its chlorine content, affects the annealing behaviour of fission tracks (Green et al., 1986, and others). In general, chlorine-rich apatites anneal at higher temperatures than fluorine-rich apatites. The Laslett et al. (1987) model is based on the annealing kinetics of Durango apatite, which has a chlorine content of 0.43 wt.%. Strictly spoken, the Laslett et al. (1987) annealing model only applies for apatites with the same chemical composition as the Durango apatite. In practical use, it has turned out to yield reliable results for fluor-apatites (< 0.5 wt.% Cl), whereas chlorine-apatites potentially cause problems. For this reason, we checked the chemical compositions of 196 apatites from 10 samples of the Donets Basin using microprobe analysis. The analysed grains were the same which were previously used for FT analysis. For analytical details we refer to Appendix A. The results are shown in Fig. 7. Average chlorine contents range between

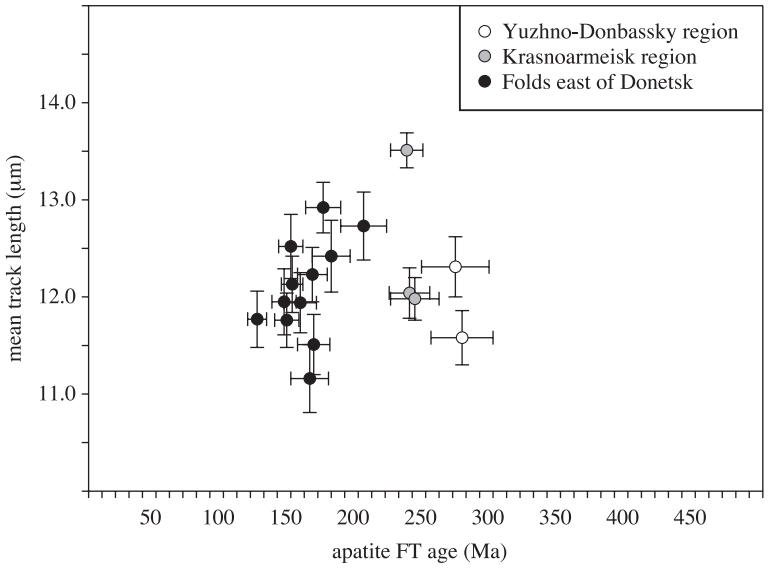

Fig. 6. "Boomerang plot" (Green, 1986): relationship between FT age and mean FT length ($\pm 1\sigma$). The pattern of the plot implies a complex cooling history for the samples of the Donbas Foldbelt.

0.09 and 0.47 wt.%. Therefore, the modelled thermal histories based on the Laslett et al. (1987) annealing data should yield reasonable estimates.

(2) The Laslett et al. (1987) model is known to underestimate low-temperature annealing, i.e., shortening of tracks that takes place at temperatures around and below 60 °C (e.g. Vrolijk et al., 1992). To adjust the modelling results to the observed amount of annealing, the model requires an artificial, late cooling event. This effect can be avoided by reducing the initial track length value (Kohn et al., 2002, Gunnell et al., 2003). The Laslett et al. (1987) annealing model uses an initial (i.e., unshortened) track length of 16.3 μm which corresponds to the mean lengths of tracks induced by thermal neutron irradiation in a nuclear reactor. Naturally occurring spontaneous tracks, however, normally do not exceed mean lengths of 14.5–15 μm (Gleadow et al., 1986). Gunnell et al. (2003) demonstrated that using an initial track length of 14.5 μm yields thermal histories which are in good agreement with independently established geological information. Therefore, we adopted an initial track length of 14.5 μm for modelling time–temperature paths for samples of the Donets Basin.

This study combines thermal history models deduced from fission track data and from vitrinite reflectance data. The latter are based on 1D numerical modelling of coalification profiles from boreholes and reveal information on the heat-flow history of the respective well. Techniques and input parameters were described by Sachsenhofer et al. (2002). The use of two different types of models may be puzzling. To avoid confusion, we refer in the following to modelling of coalification data as "VR numerical modelling", and to modelling of fission track data as "FT thermal modelling".

3.4.1. Folds east of Donetsk

We assume similar trends for the thermal histories of all samples of this area (Don 4–18). The following independent information can potentially be incorporated in the FT thermal modelling: Maximum burial occurred during Sakmarian times (~ 280–270 Ma), followed by an erosion period during the late Permian (ca. 4–5 km of denudation, Nagorny and Nagorny, 1976; Sachsenhofer et al., 2002). Zr FT dating and VR numerical modelling (Sachsenhofer et al., 2002) suggest a heating event at ~ 250 Ma. Zr FT data showed that maximum heating of the samples, as reflected by VR data, took place during this Permo-Triassic event. Hence, cooling following the Permo-

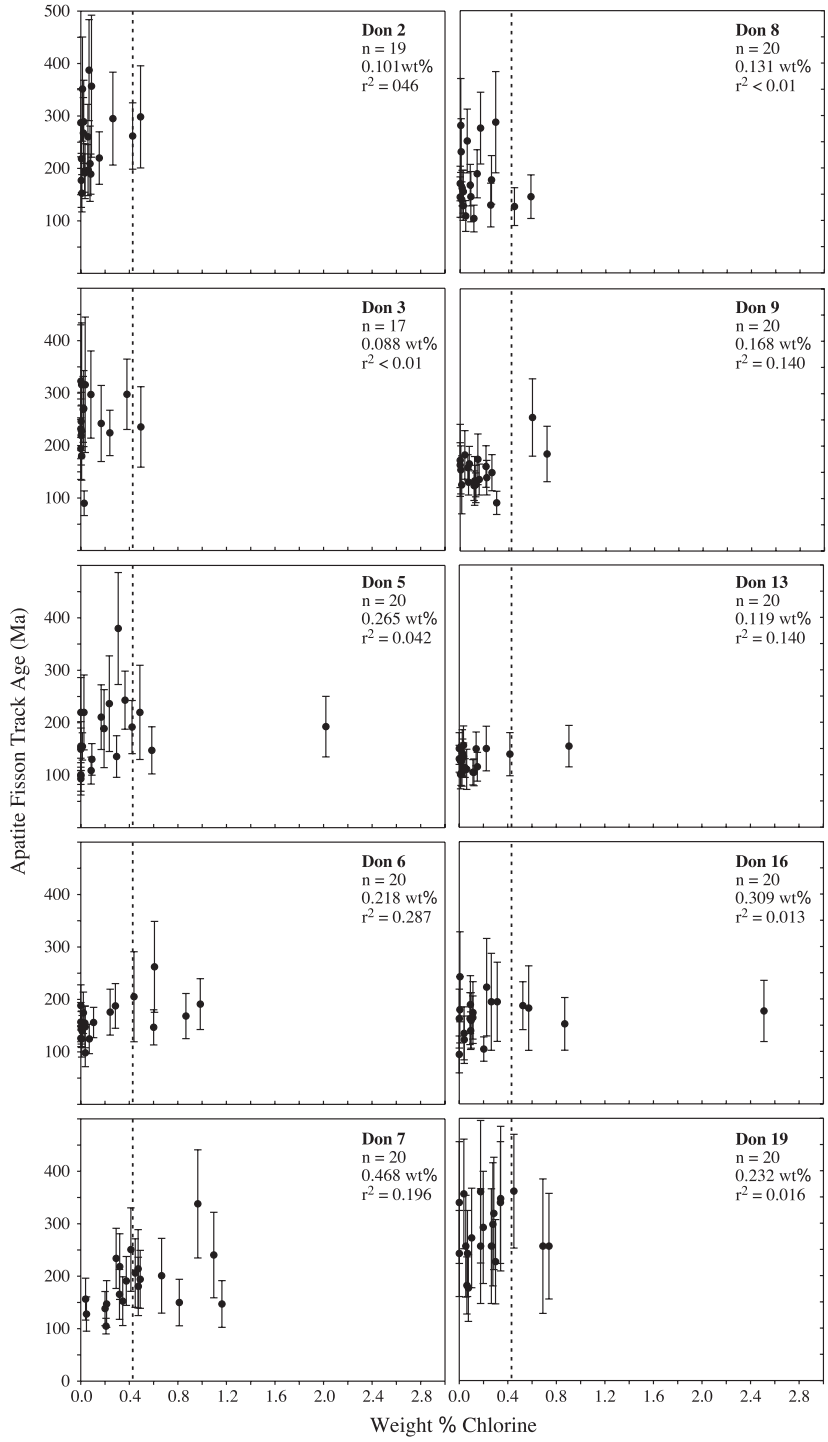

Fig. 7. Cl contents of apatites, plotted against their FT ages. The dashed lines refer to the Cl content of Durango apatite (0.43 wt.%). Right upper corner: Sample code, number of probed apatite grains, average Cl content of the sample, correlation coefficient between FT age and Cl content.

Triassic event is the earliest thermal information recorded by the apatite FT system. All information on the earlier thermal history has been overprinted by the Permo-Triassic high heat flow event. Because of the sparse sedimentary record only little is known about the Mesozoic subsidence and denudation history of the basin. For the FT thermal modelling we followed two approaches:

(1) For the "free" approach, only two constraints were set: the time and temperature of maximum heating deduced from VR and Zr FT data as starting point of the time–temperature path, and the present-day temperature as its end. This approach yields good to acceptable results for all samples. Modelled time–temperature paths for three selected samples are shown in Fig. 8A. According to this approach all samples experienced very slow, single-staged cooling. They all stayed within temperatures of the PAZ during most of the Jurassic and parts of the Cretaceous, leaving the PAZ during the Cretaceous (between 115 and 84 Ma). During their stay in the PAZ the average cooling rate was in the range of 0.4–0.7 °C/Ma.
(2) To test more complex, multi-stage thermal histories we used forward modelling for all samples (Ketcham et al., 2000). The time–temperature paths attained by this process were used as constraints for another run of inverse modelling. This yields thermal histories which are consistent with all samples. They involve cooling to temperatures around or below 60 °C after Permo-Triassic maximum heating, followed by a late Jurassic to early Cretaceous reheating to temperatures around 100 °C, and a final cooling below 60 °C during the Cretaceous (Fig. 8B). Compared to the single-stage cooling of the "free" approach, these thermal histories yield slightly improved fits, particularly in terms of the high standard deviations of the mean track lengths.

Time–temperature paths deduced from FT thermal modelling were integrated into the VR numerical modelling of well S-1379 (see Fig. 1) in order to test whether the FT-based cooling paths agree with VR trends. Both potential thermal histories, the single-stage cooling model and the multi-stage cooling model, match the VR data (Fig. 9). The single-stage cooling model requires a long continuous decrease in heat flow following the Permo-Triassic heating event (Fig. 9A) and a major early Cretaceous exhumation phase. In contrast, the multi-stage cooling model requires a separate Jurassic heating phase related to a heat flow in the range of 90 mW/m^2 (Fig. 9B). A Jurassic reheating is in line with Jurassic magmatic activity in the basin. Therefore, and because of the slightly better fit with the observed standard deviations of the mean track lengths, we favour the multi-stage cooling model. However, without additional geological evidence for the Mesozoic denudation history, we cannot ultimately decide which cooling model is closer to the "true story".

The following conclusions apply for both models: (i) the samples from the area east of Donetsk stayed at elevated temperatures within the PAZ during most of the Jurassic, (ii) cooling was a slow process with average cooling rates in the range of or below 1 °C/Ma, and (iii) all samples cooled to temperatures below 60 °C during the Cretaceous (~120–80 Ma) and have not been reheated since then.

3.4.2. Krasnoarmeisk Monocline

For the region of the Krasnoarmeisk Monocline again different potential time–temperature evolutions have been tested by FT thermal modelling and by VR numeric modelling:

(1) For the first approach we assumed that the samples experienced maximum heating at ~250 Ma, similar to the samples from the region east of Donetsk. This is not very likely because the tail of strongly shortened tracks imply a prolonged stay at elevated temperatures within in the PAZ. On the other hand, for reproducing the Triassic FT ages the samples must have cooled to temperatures below the PAZ shortly after the Permo-Triassic heating event. As expected, modelling for this approach yields a poor fit of predicted and observed data. Therefore, we assume that maximum heating, as reflected by the VR data, was coeval with maximum burial, i.e., at about 280–270 Ma during the Sakmarian (Sachsenhofer et al., 2002).

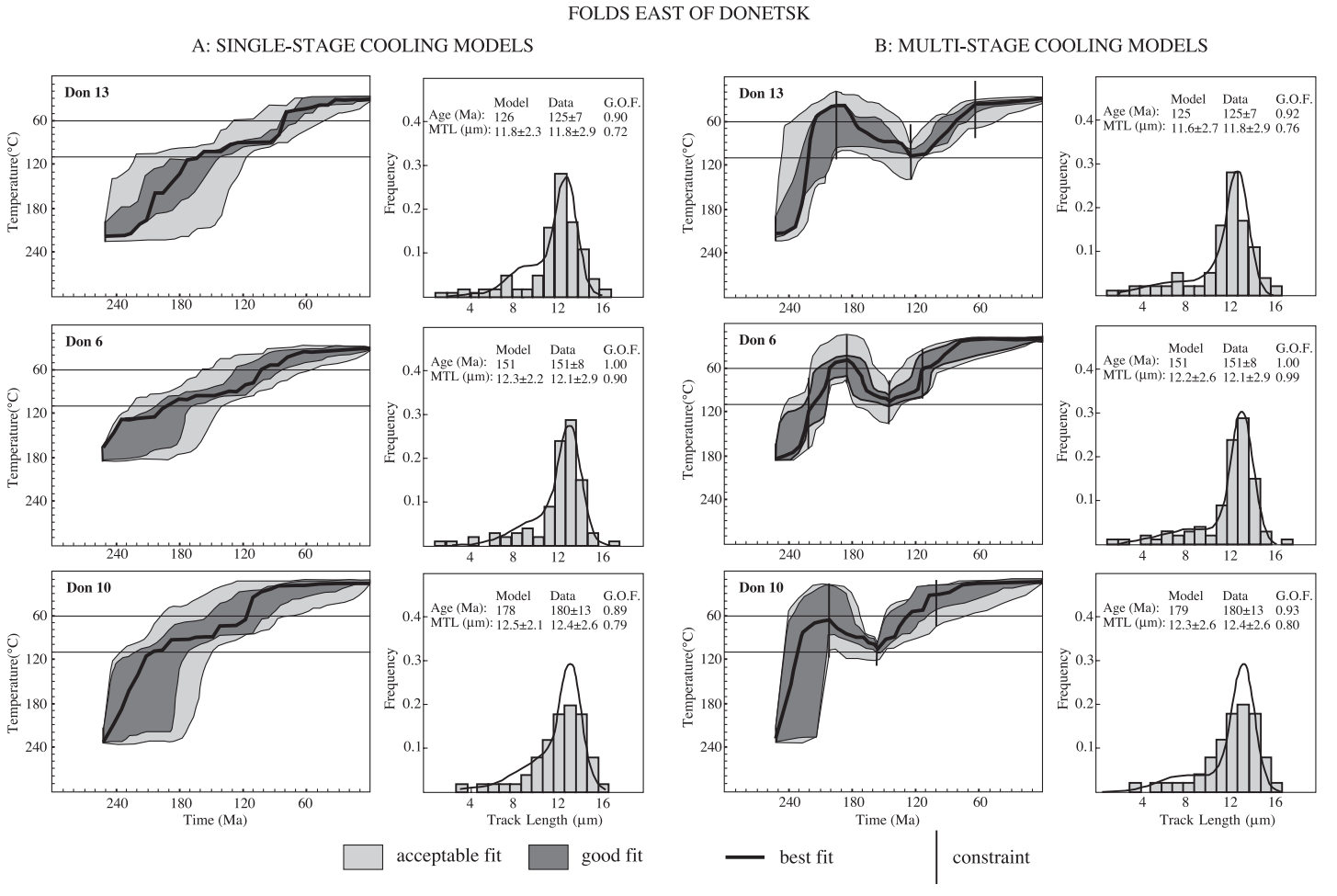

Fig. 8. FT thermal models for three selected samples from the folds east of Donetsk. For (A), a simple single-staged cooling path is assumed. (B) suggests a more complex thermal history, involving an early cooling period and a late Jurassic/early Cretaceous reheating. Both models are consistent with the FT data. See text for discussion.

(2) The Sakmarian maximum burial was followed by about 2–3 km of erosion during the late Permian (Nagorny and Nagorny, 1976; Sachsenhofer et al., 2002). We used VR numerical models of well K-1517 for estimating the amount of cooling in response to erosion (Fig. 9C). (i) Assuming that the 250 Ma high heat flow event did not affect the Krasnoarmeisk Monocline at all, Permian erosion

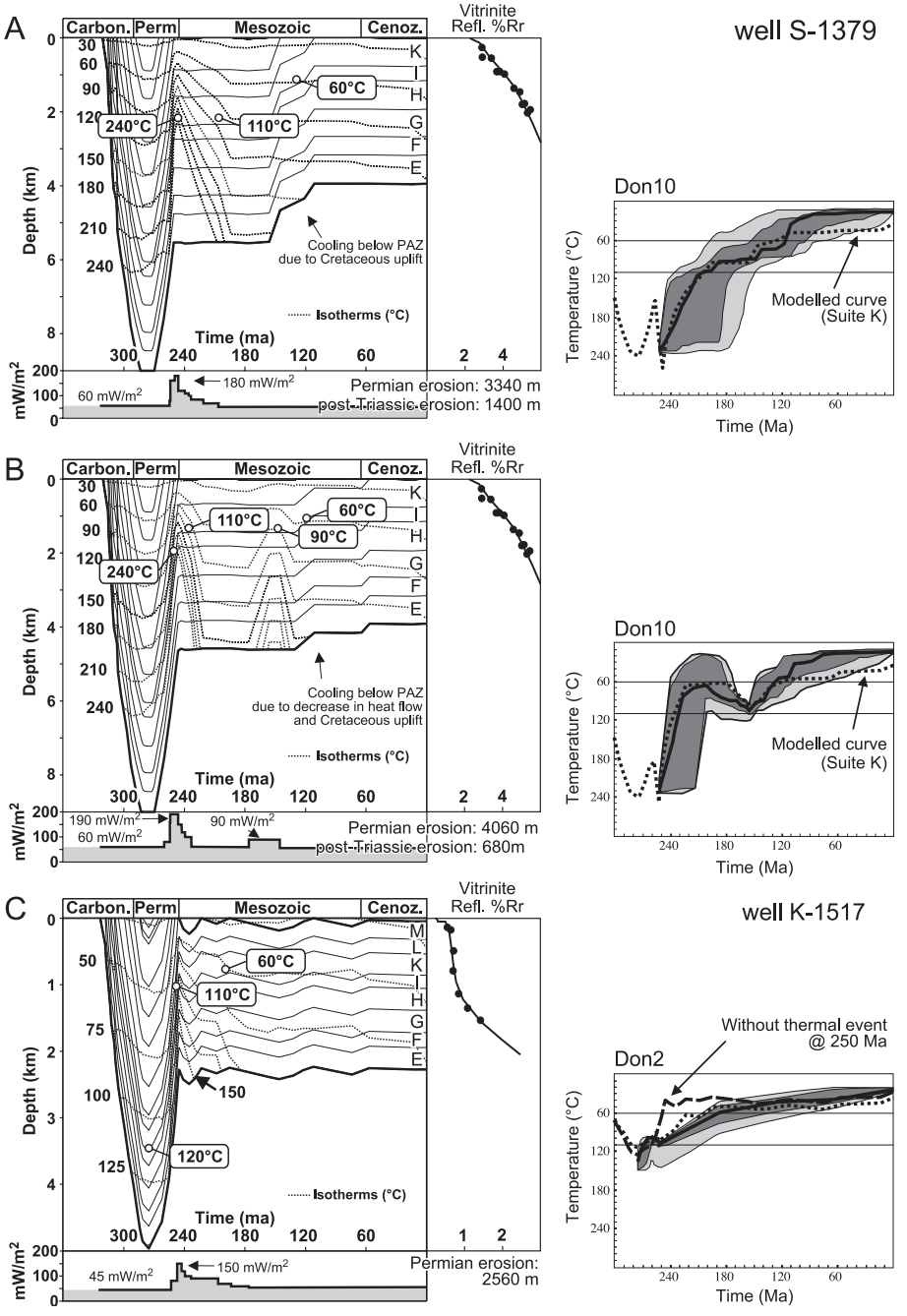

would have caused cooling in the range of 80–90 °C. For example, if Don 2 experienced temperatures of 120–150 °C during Permian maximum burial, late Permian erosion would have caused the sample to cool to temperatures between approximately 35 and 65 °C (Fig. 9C). This in turn means that the samples of the Krasnoarmeisk Monocline would have cooled below the PAZ as early as late Permian/early Triassic. The shortened track lengths, however, require a longer stay in the PAZ. Accordingly, FT thermal modelling based on maximum temperatures during the Sakmarian followed by a late Permian cooling of 80–90 °C yields poor results. Alternatively, we tried to reproduce the shortened lengths by introducing a heating event during the Jurassic, but this approach results in FT ages which are much too young. (ii) If we assume that the 250 Ma high heat flow event caused a reheating, then the late Permian erosion would only result in a cooling of about 10–20 °C (Fig. 9C). Modelling this thermal history yields good results (Fig. 10A) and leads to the following conclusions:

(i) The samples of the Krasnoarmeisk Monocline experienced maximum heating coeval with maximum burial at about 280–270 Ma, (ii) cooling associated with late Permian erosion was only in the range of 10–20 °C, (iii) the 250 Ma high heat flow event caused reheating to temperatures of about 100 °C, (iv) reheating was followed by slow cooling with an average rate of <1 °C/Ma during the Triassic, and (v) the samples finally cooled below temperatures of the PAZ during early to mid-Jurassic times.

3.4.3. Yuzhno–Donbassky region

For samples from the Yuhno–Donbassky region we again assume that maximum heating was coeval with maximum burial (280–270 Ma). No coalification profile and accordingly no VR numeric model is available from this area. However, in accordance with results from a neighbouring borehole 15 km to the north (Sachsenhofer et al., 2002), we assume that late Permian erosion was in the range of 2.5 km, associated with ca. 40 °C of cooling. Good fits for the FT thermal modelling are obtained using these constraints (Fig. 10B). According to FT thermal modelling, the Permo-Triassic heat flow event only caused a slight reheating, if any. Temperatures at 250 Ma were in the range of about 80–85 °C. After 250 Ma, the samples slowly cooled to temperatures below 60 °C, leaving the PAZ during the mid-Jurassic.

Near the location of sample Don 19, coaked coal occurs at the contact to Permian sills and dikes (e.g. Jernovaya, 1997), which intruded during early basin uplift (e.g. Buturlinov, 1964). It is questionable, whether the magmatic bodies resulted in a regional increase in heat flow and temperatures (see Sachsenhofer et al., 2002). In any case, if it caused any thermal perturbance, its influence cannot be distinguished from the thermal overprint caused by deep Permian burial.

The Yuzhno–Donbassky region is located close to the former Permian basin margin. Therefore, a slightly earlier start of exhumation ($\sim$285 Ma) cannot be excluded. Sensitivity analyses have shown that the assumption of an Asselian maximum burial does not change any of our conclusions.

Fig. 9. Integration of vitrinite reflectance (VR) and fission track (FT) data. Left-hand side: VR numerical modelling of subsidence and heat flow history, taking into account FT thermal models shown on the right. Measured (dots) and calculated (lines) VR data are shown. Right-hand side: Time–temperature path for suite K according to VR numerical modelling (dotted line) and thermal histories for samples Don 10 and Don 2 according to FT thermal modelling (see Figs. 9 and 11). See Fig. 2 for position of key-wells. (A) Well S-1379: Results of VR numerical modelling on the basis of a single-stage cooling history, revealing a slow decrease in heat flow after the Permo-Triassic heat flow event and a major early Cretaceous exhumation phase. Temperature estimates for samples Don 14 (240 °C) and Don 10 are shown in boxes. (B) Well S-1379: Results of VR numerical modelling on the basis of a multi-stage cooling history, revealing a Jurassic heat flow event (90 mW/m^2). Temperature estimates for samples Don 14 (240 °C) and Don 10 are shown in boxes. Both models (A and B) result in good fits between the temperature path of suite K from well S-1379 and the results of Don 10 (suite K; Fig. 8B). (C) Well K-1517: Results of VR numerical modelling on the basis of FT thermal models shown in Fig. 10. The heat flow decreases gradually following the Permo-Triassic heating event. Temperature estimates for sample Don 2 are shown in boxes. Right-hand side: Two different time–temperature curves deduced from VR numerical modelling for suite K in well K-1517 (dotted lines) are shown in comparison to the results of FT thermal modelling of Don 2 (suite K; Fig. 10A). A model without a Permo Triassic heating event (dashed line) results in a Permian temperature maximum and a subsequent fast cooling, which is not observed in the FT thermal modelling of Don 2. In contrast, a Permo Triassic heating event results in a good fit (dotted line).

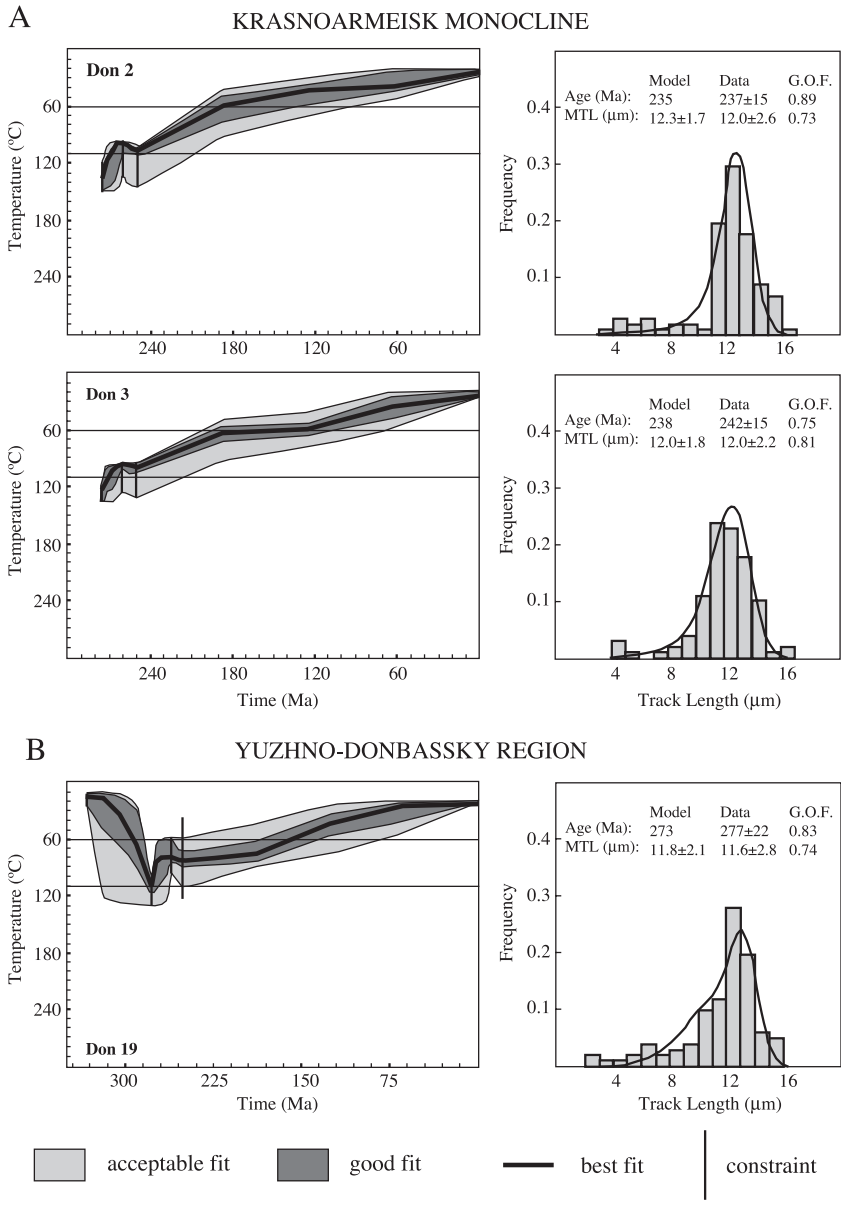

Fig. 10. FT thermal models for the Krasnoarmeisk Monocline (A), and the Yuzhno–Donbassky region (B).

3.5. Cretaceous cooling paths: tectonic implications

Modelling of the FT data reveals that the studied samples cooled below 60 °C between 220 and 80 Ma. Within the folds east of Donetsk, the precise cooling ages depend on whether a single-stage cooling path (Fig. 8A) or a multi-stage thermal history (Fig. 8B) is assumed.

Modelled ages of cooling below temperatures of the PAZ considering a Jurassic thermal event are displayed in Fig. 11. Obviously, samples from the southern Donbas (Yuzhno–Donbassky region) and the western Krasnoarmeisk Monocline cooled below 60 °C during Jurassic times. Modelled cooling ages from the area east of Donetsk vary from 140 to 80 Ma. Some ages are plotted along a cross-section in

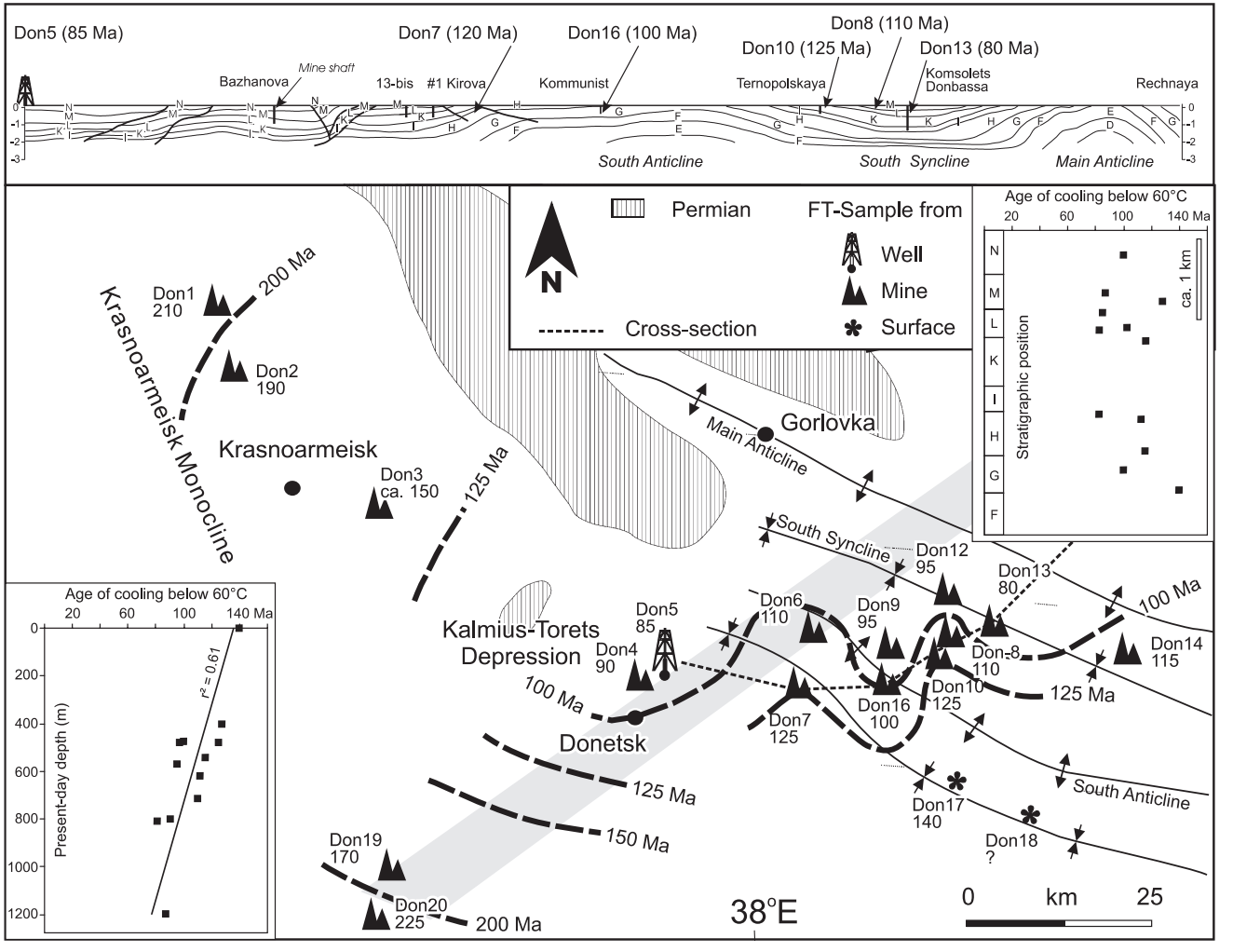

Fig. 11. Map showing cooling ages (cooling below 60 °C) derived from models shown in Fig. 8B (multi-stage cooling with Jurassic reheating). Isolines are hand-contoured. Insets show a geological cross-section and plots of cooling ages versus stratigraphic position of the samples and versus present-day depth. (Only data from the folds east of Donetsk are considered in the cross-plots.)

Fig. 11. The sketch suggests that cooling ages are not correlated with the position of the samples along synclines or anticlines. Although samples from suites G–H display generally higher ages than samples from suites K–N, there is no clear trend between cooling ages and the stratigraphic position of the samples. However, a fair correlation (correlation coefficient $r^2 = 0.61$) exists between cooling ages and the present-day depth of the samples (insets in Fig. 11). This suggests that the formation of the South Syncline and the South Anticline pre-dates Cretaceous cooling and argues against a late Cretaceous age of folding. It is important to note that, depending on the applied cooling path (single- or multi-stage), the reconstructed cooling ages differ by up to 20 Ma. Nevertheless, the trends and interpretations remain the same.

A pre-Cretaceous age of folding is in agreement with the traditional concept of a Permian compressional event. Saintot et al. (2003b) speculate that the development of the folds was controlled by Permian transtension and salt tectonics. The latter hypothesis is also in agreement with the FT data. Moreover, folding may be related to a late Triassic/early Jurassic compressional event.

Whereas the open folds south of the Main Anticline were formed during Permian and/or Triassic/Jurassic (Cimmerian) times, late Cretaceous compressional structures are well established along the northern basin margin (e.g. Popov, 1963; Saintot et al., 2003a,b). Vertical movements related to this late tectonic activity had little effect on the thermal evolution of the studied rocks.

3.6. Relationships of the thermotectonic evolution of the Donbas with the evolution of the southern margin of the Eastern European Craton

Milestones of the thermal evolution of the Donbas Foldbelt include a Permo-Triassic heating event, a subordinate heat flow event during Jurassic time and/or Cretaceous cooling due to uplift.

The Permo-Triassic event with heat flows up to 200 mW/m^2 seems to be related to magmatic activity. Contemporanous magmatic activity in the Donbas Foldbelt and the Scythian platform suggest a common deep magmatic source (Alexandre et al., 2003). Thus, it is likely that the area with high heat flow was not restricted to the Donbas Foldbelt. Probably, large parts of the southern margin of the Eastern European Craton were affected by high heat flows during late Permian/early Triassic times. This is also supported by early/middle Triassic magmatic rocks in the Karpinsky Swell (e.g. Nikishin et al., 2002). The latter authors speculate that magmatic activity and rifting reflect the build-up of regional extensional stresses in Euroasia and are related to a global reorganization of plate boundaries.

Samples east of Donetsk, including surface sample Don 17 suffered temperatures in the order of 90–100 °C during Jurassic times. The VR numeric models show that the high temperatures were caused by high Jurassic heat flows (Fig. 9B) and/or a deep position of the samples during Jurassic times. In the latter case, the reconstructed cooling paths argue for a considerable Cretaceous exhumation (Fig. 9A/B). High Jurassic heat flow is in accordance with coeval magmatic activity in the Donbas Foldbelt. Independent support for a Jurassic heating event is provided by subsidence models for the North Caucasus Basin (Scythian Platform). Using tectonic subsidence curves, Ershov et al. (2003) observed a significant early Jurassic uplift phase. According to these authors, uplift was a consequence of the heating of the lithosphere underneath the Scythian Platform by numerous intrusions. Although magmatic activity in the Donbas Foldbelt is slightly younger, magmatic activity and the observed high temperatures may be related to the intrusive warming.

4. Conclusion

Using VR data and 1D and 2D thermal models, Sachsenhofer et al. (2002) reconstructed a complicated thermal history involving thermal events with heat flows up to 200 mW/m^2. The zircon and apatite FT data provide new information, which expands the knowledge of the thermotectonic evolution of the Ukrainian Donbas Foldbelt significantly:

- Folds NE of Donetsk: Zircon FT ages (250 Ma) confirm a Permo-Triassic heat flow event, which postdates maximum Permian burial. Heating was caused by magmatic activity reflecting extensional stresses which affected the southern margin of the Eastern European Craton.

- Apatite FT data yield additional information on the younger history of the basin. Jurassic temperatures were in the order of 90–100 °C. These relatively high temperatures imply that a significant part of the Carboniferous sequence became eroded only during early Cretaceous time and/or that Jurassic heat flow was increased. Increased Jurassic heat flow may be related to heating of the lithosphere, which caused uplift and erosion along the northern margin of the Scythian Platform.
- Krasnoarmeisk Monocline: Heating events in the Krasnoarmeisk Monocline were related to Permian maximum burial and to Permo-Triassic magmatic activity. The extent of the area with a Permo-Triassic heating is larger than previously assumed. After the Permo-Triassic event, heat flow decreased slowly.
- Main heating within the Yuzhno–Donbassky region (SW Donetsk) occurred during deep Permian burial. Permian alkaline magmatism had little influence on the regional heat flow.
- Sediments in the southern Donbas (Yuzhno–Dobassky region) and the westernmost Krasnoarmeisk Monocline cooled below 60 °C during Jurassic times. Sediments northeast of Donetsk cooled below 60 °C only during Cretaceous times. The spatial distribution of the cooling ages suggests that the formation of the South Syncline and the South Anticline predates Cretaceous cooling.

Acknowledgements

The authors would like to express their gratitude to staff member from the coal mines for providing samples and additional geological information. Financial support by the Austrian Science Foundation (FWF project no. 14895), the German Science Foundation (grant SP 673/1-1) and the state of Baden-Württemberg (Postdoktorandenförderung der Landesstiftung) is gratefully acknowledged. The paper benefited from discussions with A. Saintot, R. Stephenson (Amsterdam), B. Panov (Donetsk) and A. Kitchka (Kiev) on different aspects of the evolution of the Donbas. C.S. thanks the members of the Melbourne thermochronology group, especially Asaf Raza, Matevs Lorencak and Barry Kohn, for the introduction to the lab facilities of the Melbourne University and for stimulating discussions. Thanks also to Craig Schneider and Ursula Weber for proofreading the manuscript. Critical reviews by P. O'Sullivan and S. Stovba are gratefully acknowledged.

Appendix A. Analytical details

A.1. FT analysis

The samples were crushed, sieved (fraction 63–250 μm) and processed by standard heavy liquid and magnetic separation techniques. Apatites were mounted in epoxy resin, zircons in PFA Teflon. At least two mounts per sample were used for Zr FT analysis. The mineral mounts were grinded and polished to reveal internal surfaces. Apatites were etched for 20 s in 5 M HNO_3 at room temperature, zircons for 7–13 h in a KOH–NaOH–LiOH eutectic melt at 190 °C. Thermal neutron irradiation was carried out at the HIFAR reactor facility in Lucas Heights, Australia. FT dating was performed according to the external detector method (Gleadow, 1981) and the zeta calibration approach (Hurford and Green, 1983). Mica detectors were etched in HF (40%) for 35 min at room temperature. FT ages were calculated using a zeta value of 390 ± 6 for apatite (CN5 dosimeter glass), and of 116 ± 2 for zircon (CN2 dosimeter glass). Tracks were counted under a Zeiss Axiotron optical microscope with dry objectives and 1250× magnification for apatite FT analysis and 1600× magnification for zircon FT analysis. FT ages were calculated by the Trackkey program (Dunkl, 2002).

A.2. Microprobe analysis

Microprobe analysis have been carried out at Geotrack International, Australia. The Chlorine contents of 196 apatite grains from 10 samples have been measured, using a JEOL JXA-5A electron microprobe at 15 kV accelerating voltage, a beam current of 29 nA and a beam diameter of 15–20 μm.

References

Aleksandrov, A.L., Gordienko, V.V., Derevskaya, K.I., Zemskov, G.A., Ivanov, A.P., Panov, B.S., Shumlyanskiy, V.A., Epov, O.G., 1996. Deep Structure, Evolution of Fluid Systems and Endogenic Gold-Bearing Potentiality, South-Eastern part of

Ukrainian Donets Basin (in Russian). Edition of Institute of Fundamental Researches of Ukrainian Scientific Association, Kyiv. 74 pp.

Alexandre, P., Saintot, A., Wiljbrans, J., Stephenson, R., Wilson, M., Kitchka, A., Chalot-Prat, F., 2003. $^{40}Ar/^{39}Ar$ dating of magmatic activities in the Donbas Foldbelt and the Scythian Platform (Eastern Europe) indicating a possible mantle plume source. Geophys. Res., 5.

Belokon, V.G., 1971. Geological history of evolution of the Donbas (in Russian). Geology and Prospecting of Coal Deposits. Nedra, Moscow, pp. 3–15.

Belokon, V.G., 1975. Deep structure of the Donbas (in Russian). Geol. J. 5, 11–27.

Burnham, A.K., Sweeney, J.J., 1989. A chemical kinetic model of vitrinite maturation and reflectance. Geochim. Cosmochim. Acta 53/10, 2649–2657.

Buturlinov, N.V., 1964. Main features of petrochemistry of magmatic rocks of the Donets Basin (in Russian). Reports Ac. Sc. USSR 157 (2), 357–360.

Chekunov, A.V., 1994. The geodynamics of the Dniepr–Donets Rift (in Russian). Geophys. J. 16, 3–13.

de Boorder, H., van Beek, A.J.J., Dijkstra, A.H., Galetsky, L.S., Koldewe, G., Panov, B.S., 1996. Crustal architecture of the Donets Basin: tectonic implications for diamond and mercury–antimony mineralization. Tectonophysics 268, 293–309.

Dunkl, I., 2002. Trackkey: a windows program for calculation and graphical presentation of fission track data. Comput. Geosci. 28, 3–12.

Einor, O.L., 1996. The former USSR. In: Wagner, R.H. (Ed.), The Carboniferous of the world III, The former USSR, Mongolia, Middle Eastern Platform, Afghanistan, and Iran. IUGS Publ., vol. 33. Instituto Geologico y Minero de Espana, Madrid, pp. 13–407.

Ershov, A.V., Brunet, M.-F., Nikishin, A.M., Bolotov, S.N., Nazarevich, B.P., Korotaev, M.V., 2003. Northern Caucasus basin: thermal history and synthesis of subsidence models. Sediment. Geol. 156, 95–118.

Galbraith, R.F., 1990. The radial plot: graphical assessment of spread in ages. Nucl. Tracks Radiat. Meas. 17, 207–214.

Gallagher, K., Brown, R.W., Johnson, C.J., 1998. Geological applications of fission track analysis. Annu. Rev. Earth Planet Sci. 26, 519–572.

Gavrish, V.K. (Ed.), 1989. Geology of Oil and Gas Potential of the Dniepr–Donets Depression: Depth Structure and Geotectonic Evolution (in Russian). Naukova Dumka, Kiev. 208 pp.

Gleadow, A.J.W., 1981. Fission track dating methods: what are the real alternatives? Nucl. Tracks Radiat. Meas. 5, 3–14.

Gleadow, A.J.W., Duddy, I.R., 1981. A natural long-term annealing experiment for apatite. Nucl. Tracks Radiat. Meas. 5, 169–174.

Gleadow, A.J.W., Duddy, I.R., Green, P.F., Lovering, J.F., 1986. Confined fission track lengths in apatite: a diagnostic tool for thermal history analysis. Contrib. Mineral. Petrol. 94, 405–415.

Grad, M., Gryn, D., Guterch, A., Janik, T., Keller, R., Lang, R., Lyngsie, S.B., Omelchenko, V., Starostenko, V.I., Stephenson, R.A., Stovba, S.M., Thybo, H., Tolkunov, A., 2003. "DOBREfraction '99"—velocity model of the crust and upper mantle beneath the Donbas Foldbelt (East Ukraine). Tectonophysics 371, 81–110.

Green, P.F., 1986. On the thermo-tectonic evolution of Northern England: evidence from fission track analysis. Geol. Mag. 123, 493–506.

Green, P.F., Duddy, I.R., Gleadow, A.J.W., Tingate, P.R., Laslett, G.M., 1986. Thermal annealing of fission tracks in apatite: 1. A qualitative description. Chem. Geol. 59, 237–253.

Gunnell, Y., Gallagher, K., Carter, A., Widdowson, M., Hurford, A.J., 2003. Denudation history of the continental margin of western peninsular India since the early Mesozoic—reconciling apatite fission-track data with geomorphology. Earth Planet. Sci. Lett. 215, 187–201.

Harland, W.B., 1990. A Geologic Time Scale 1989. Cambridge Univ. Press, Cambridge. 263 pp.

Hurford, A., 1986. Cooling and uplift patterns in the Lepontine Alps, South Central Switzerland, and an age of vertical movement on the Insubric fault line. Contrib. Mineral. Petrol. 92, 412–427.

Hurford, A.J., Green, P.F., 1983. The zeta age calibration of fission track dating. Chem. Geol. 41/4, 285–317.

Izart, A., Le Nindre, Y., Stephenson, R., Vaslet, D., Stovba, S., 2003. Quantification of the control of sequences by tectonics and eustacy in the Dniepr–Donets Basin and on the Russian Platform during Carboniferous and Permian. Bull. Soc. Géol. Fr. 174, 93–100.

Jernovaya, G., 1997. Thermally metamorphosed coals from the southern Donbas, Ukraine. In: Proceedings of the XIII Int. Congress on the Carboniferous and Permian. Polish Geological Institute, Warsaw, pp. 75–78.

Ketcham, R., Donelick, R., Donelick, M., 2000. AFTSolve: a program for multi-kinetic modeling of apatite fission track data. Geol. Mater. Res. 2/1, 1–18.

Kohn, B.P., Gleadow, A.J.W., Brown, R.W., Gallagher, K., O'Sullivan, P.B., Foster, D.A., 2002. Shaping the Australian crust over the last 300 million years: insights from fission track thermotectonic imaging and denudation studies of key terranes. Aust. J. Earth Sci. 49, 697–717.

Laslett, G., Green, P., Duddy, I., Gleadow, A., 1987. Thermal annealing of fission tracks in apatite. Chem. Geol. 65, 1–13.

Lazarenko, E.K., Panov, B.S., Gruba, V.I., 1975. The Mineralogy of the Donets Basin, 1 (in Russian) Naukova dumka, Kiev. 225 pp.

Levenshtein, M.L., Spirina, O.I., Nosova, K.B., Dedov, V.S., 1991. Map of coal Metamorphism in the Donetsk Basin (Paleozoic surface). 1:500.000. Ministry of Geology of the USSR, Kiev.

Lutugin, L.I., Stepanov, P.I., 1913. Donets Coal basin. Review of Coal Deposits of Russia. Geolkom (Geological Committee of Russia), St. Petersburg.

Maystrenko, Y., Stovba, S., Stephenson, R., Bayer, U., Menyoli, E., Gajewski, D., Huebscher, C., Rabbel, W., Saintot, A., Starostenko, V., Thybo, H., Tolkunov, A., 2003. Crustal-scale pop-up structure in cratonic lithosphere: DOBRE deep seismic reflection study of the Donbas fold belt, Ukraine. Geology 31, 733–736.

McCann, T., Saintot, A., Chalot-Prat, F., Kitchka, A., Fokin, P., Alekseev, A., Europrobe-intas Research Team, 2003. Evolution of the southern margin of the Donbas (Ukraine) from Devonian

to Early Carboniferous times. In: McCann, T., Saintot, A. (Eds.), Tracing Tectonic Deformation Using the Sedimentary Record-Geological Society of London, Special Publication, vol. 208, pp. 117–135.

Mikhalyev, A.K., 1976. The mechanism of thrust formation and peculiarities of the evolution of the Donets Basin (in Russian). In: Pogrebnov, N.I. (Ed.), Tectonics of Coal Basins and Deposits of the USSR. Nedra, Moscow, pp. 102–106.

Nagorny, Yu.N., 1971. On folding of alpine tectonogenesis in the Donbas (in Russian). Geology and Prospecting of Coal Deposits. Nedra, Moscow, pp. 62–70.

Nagorny, Yu.N., Nagorny, V.N., 1976. Peculiarities of geological evolution of the Donets Basin (in Russian). Geotectonics 1, 74–86.

Nesterenko, L.P., 1978. Early Permian Deposits of the Kalmius–Torets Depression in the Donets Basin (in Russian). Vischa shkola, Kiev. 148 pp.

Nikishin, A.M., Ziegler, P.A., Abbott, D., Brunet, M.-F., Cloetingh, S., 2002. Permo-Triassic intraplate magmatism and rifting in Eurasia: implications for mantle plumes and mantle dynamics. Tectonophysics 351, 3–39.

Pogrebnov, N.I., 1971. History of tectonic movements and sedimentation in the Eastern part of the Great Donbas (in Russian). Geology and Prospecting of Coal Deposits. Nedra, Moscow, pp. 15–24.

Popov, V.S., 1963. Tectonics of the Donbas (in Russian). In: Kuznetzov, I.A. (Ed.), Geology of Coal Deposits and Coaly Shales of the USSR, vol. 1. Gosgeoltehnauchizdat, Moscow. 1201 pp.

Popov, V.S., 1966. Coalification Map of the Ukrainian Donbass. 1:500.000. Ministry of Geology of the USSR, Kiev.

Privalov, V.A., 1998. Block rotations and scenario of the tectonic evolution of the Donets Basin (in Russian). Geology and Geochemistry of Fossil Fuel Deposits, vol. 105 (4). National Academy of Science, Institute of Geology and Geochemistry of Fossil Fuels, Lwov, pp. 142–158.

Privalov, V.A., 2000. Local extension as factor governing the localisation of centres of magmatism and endogenous mineralization in the Donbas (in Russian).Transactions of Donetsk State Technical University (Trudi DonGTU), 11, 115–120.

Privalov, V.A., Panova, E.A., Azarov, N.Ya., 1998. Tectonic events in the Donets Basin: spatial, temporal and dynamic aspects (in Russian). Geology and Geochemistry of Fossil Fuel Deposits, vol. 105 (4). National Academy of Science, Institute of Geology and Geochemistry of Fossil Fuels, Lwov, pp. 11–18.

Privalov, V.A., Zhykalyak, N.V., Ovcharenko, V.A., Panova, E.A., 2002. Magnitudes of different aged displacements for regional faults of northern margin of the Donbas (in Russian). Mineralni Resursi Ukraini (Mineral Resources of Ukraine). Ministry of Ecology and Natural Resources, Ukrainian State Geological Prospecting Institute, Kiev. 2, 21–23.

Sachsenhofer, R.F., Privalov, V.A., Zhykalyak, M.V., Bueker, C., Panova, E.A., Rainer, T., Shymanovskyy, V.A., Stephenson, R.A., 2002. The Donets Basin (Ukraine/Russia): coalification and thermal history. Int. J. Coal Geol. 49, 33–55.

Sachsenhofer, R.F., Privalov, V.I., Izart, A., Elie, M., Kortensky, J., Panova, E.A., Sotirov, A., Zhykalyak, M.V., 2003. Petrography and geochemistry of Carboniferous coal seams in the Donets Basin (Ukraine): implications for paleoecology. Int. J. Coal Geol. 55, 225–259.

Saintot, A., Stephenson, R., Stovba, S., Maystrenko, Y., 2003a. Structures associated with inversion of the Donbas Foldbelt. Tectonophysics 373, 181–207.

Saintot, A., Stephenson, R., Brem, A., Stovba, S., Privalov, V., 2003b. Paleostress field reconstruction and revised tectonic history of the Donbas fold and thrust belt (Ukraine and Russia). Tectonics 22, 1059.

Sollogub, V.B., Borodulin, M.I., Chekunov, A.V., 1977. Deep structure of the Donbas and adjoining regions (in Russian). Geol. J. 2, 23–31.

Stephenson, R.A., Stovba, S.M., Starostenko, V.I., 2001. Pripyat–Dniepr–Donets Basin: implications for dynamics of rifting and the tectonic history of the northern Peri-Tethyan platform. In: Ziegler, P.A., Cavazza, W., Robertson, A.H.F., Crasquin-Soleau, S. (Eds.), Peri-Tethyan Rift/Wrench Basins and Passive Margins, Peri-Tethys Memoir 6. Mémoires du Muséum National d'Histoire Naturelle, Paris, vol. 186, pp. 369–406.

Sterlin, B.P., Makridin, V.P., Lutsky, P.I., 1963. Stratigraphy of Mesozoic and Cenozoic deposits of the Donets Basin (in Russian). Geology of Coal and Oil Shale Deposits of the USSR 1. Nedra, Moscow, pp. 64–88.

Stovba, S.M., Stephenson, R.A., 1999. The Donbas Foldbelt: its relationships with the uninverted Donets segment of the Dniepr–Donets Basin, Ukraine. Tectonophysics 313, 59–83.

Taylor, G.H., Teichmüller, M., Davis, A., Diessel, C.F.K., Littke, R., Robert, P., 1998. Organic Petrology. Gebrüder Borntraeger, Berlin. 704 pp.

van Wees, J.D., Stephenson, R.A., Stovba, S.M., Shymanovskyi, V.A., 1996. Tectonic variation in the Dniepr–Donets Basin from automated modelling of backstripped subsidence curves. Tectonophysics 268, 257–280.

Vrolijk, P., Donelick, R., Queng, J., Cloos, M., 1992. Testing models of fission track annealing in apatite in a simple thermal setting; Site 800, Leg 129. In: Larson, R., Lancelot, Y. (Eds.), Proc. ODP, Sci. Results. College Station, TX, p. 129.